

# CHARACTERIZATION OF ROMAN MORTAR FROM THE MEDIANA ARCHEOLOGICAL SITE

**Gordana A. Topličić-Čurčić, Zoran J. Grdić, Nenad S. Ristić, Dušan Z. Grdić,  
Petar B. Mitković, Igor S. Bjelić, Ana J. Momčilović-Petronijević**

## Preliminary notes

This paper presents the study of the Roman mortar used for construction of floors in the buildings which possessed floor heating system – hypocaust, in the residential villa with the peristyle (Naissus, Serbia). A total of seven samples of mortar from different locations of the villa were examined and analyzed for information about its morphological, mineralogical, chemical and basic physical properties. In order to determine these properties were used: optical microscopy, the scanning electron microscopy (SEM) with EDS analysis, X-ray diffraction analysis (XRD). The mortar is dominantly made of carbonate binder and the aggregate of grain size 0,05 to 2 mm with a rare occurrence of 10 mm grains. Fragments of mortar, grains of limestone, quartz, metamorphite and vulcanite were used for the mortar aggregate. Usage of crushed brick and reaction rim confirms its function of hydraulic binder. The weak bonds between the aggregate grains and limestone binder facilitate transport of water through the formed transit zones.

**Keywords:** optical analysis, porosity, Roman mortar, SEM-EDS, XRD, water absorption

## Karakteristike rimske žbuke s arheološkog nalazišta Mediana

### Prethodno priopćenje

Ovaj rad prikazuje istraživanje rimske žbuke rabljene za konstrukciju poda u objektima koji su imali sustav podnog grijanja – hipokaust, u rezidencijalnim vilama s peristelom (Naissus, Srbija). Ispitano je i analizirano ukupno sedam uzoraka žbuke s različitim lokacija vila s ciljem dobivanja informacija o njezinim morfološkim, mineraloškim, kemijskim i osnovnim fizikalnim karakteristikama. Za utvrđivanje ovih svojstava rabljena je: optička mikroskopija, skenirajući elektronski mikroskop (SEM), s EDS analizom, difrakcijska analiza s X-zrakama (XRD). Žbuka ima prilično ujednačene karakteristike preko cijele površine poda hipokausta. Žbuka dominantno čini karbonatno vezivo i agregat veličine zrna od 0,05 do 2 mm s rijetkom pojmom zrna dimenzija 10 mm. Kao agregat za žbuku rabljeni su dijelovi žbuke, zrna krečnjaka, kvarca, metamorfita i vulkanita. Uporaba drobljene opeke i prisustvo reakcijskog ruba, potvrđuje njezinu funkciju hidrauličnog vezivanja. Slaba veza između zrna agregata i krečnjačkog veziva omogućava transport vode kroz formiranu tranzitnu zonu.

**Ključne riječi:** optička analiza, poroznost, Rimski žbuk, SEM-EDS, XRD, upijanje vode

## 1 Introduction

The present day city of Nis occupies the location of the Roman city of Naissus, which occupied central position within Roman province Upper Moesia (Moesia Superior). The Roman Naissus was the most famous for being the birth place in 272 AD (birth dates vary but most modern historians use c. 272) of the Emperor Constantine (Flavius Valerius Aurelius Constantinus Augustus, who ruled the Roman Empire from 306 to 337 AD as 57<sup>th</sup> Emperor of Rome). In 2013 it will be 1700 years since the Edict of Milan was enacted, which was a legal act by which in 313 emperor Constantine became the first Roman ruler to have become a Christian. In the immediate proximity of Naissus, at Mediana, in times of reign of emperor Constantine, a large residential complex with a number of luxurious villas, and auxiliary structures was erected [1]. Exploration of the archeological site Mediana was started by Felix Kanitz as early as 1864 and it is recurrently undertaken until nowadays [2]. Irrespective of the importance of the site, and the needs for restoration works, until now mortar has not been researched. The most important structure on the Mediana site is the villa with the peristyle [3]. Its length is 98,6 m, and width 63 m. It has around 6800 m<sup>2</sup> of floor area, of which 945 m<sup>2</sup> were under mosaics. Besides peristyle, in the villa compound there are several areas with specific functions. The most complex function was in the northern part of the villa with audience hall, two stibadiums, thermae and several rooms where the owners of this luxurious villa used to reside. All these rooms in the north were adorned by frescoes, while the floor areas were differently finished, depending on the function they

performed. The areas of peristyle, stibadium, audience hall, thermae and the hall had floors covered by lavish mosaics. Other rooms were covered by the floors of mortar or brick. All these areas, except the porch and corridor leading to the thermae, are characterized by the specific structure underneath them – the hypocaust, Fig. 1 [4].

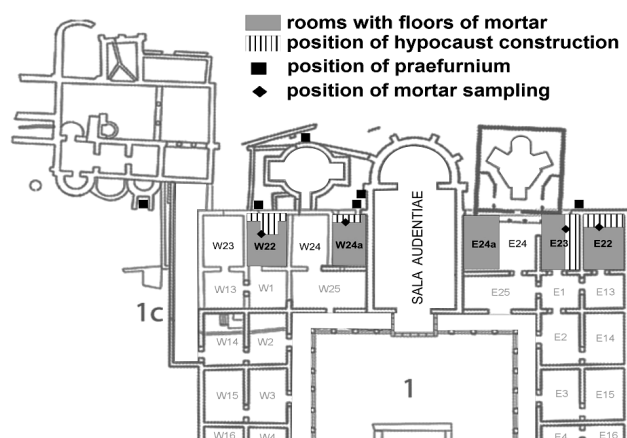


Figure 1 Northern part of Roman villa Mediana with marked position of analysed samples

Hypocaust is an ancient Roman concept for keeping the inside of buildings warm [5]. The floor heating system in Mediana testifies that the villa with the peristyle had to be equipped, for someone special, with all the fittings providing permanent comfort of its owners.

The mortar floor slabs in the villa with the peristyle at Mediana were formed using the hypocaust system model. The floor slabs over the hypocaust were heated by the hot

air created by firing wood in the covered hearth (*praefurnium*) on the outside of the heated room. Such *praefurnium* is immediately next to the wall of the heated rooms, and via the openings in its structure, the hot air expands through the structure of the hypocaust. The hypocaust in the villa with the peristyle is composed of the small pillars around 45 cm high spaced at 25 cm, made from the bricks having dimensions  $19,7 \times 19,7 \times 6$  cm. Over them were placed the larger bricks having dimensions  $56 \times 56 \times 7$  cm – the so called bipedals, which had a function of floor slab supports. It should be mentioned that in the hypocaust system at Mediana, there have been findings of fragments and traces of fresco paintings from the first phase of the villa. Also, certain systems of the hypocaust did not extend below the entire area of the floor slabs, particularly when the mortar floor slabs in the rooms in the northern half of the villa are concerned. Over the bipedals, a thick layer of mortar (10  $\div$  15 cm) mixed with small fragments of bricks was cast. The hot air that was warmed up in *praefurnium*, Fig. 2, was flowing under the floor elevated in this manner.

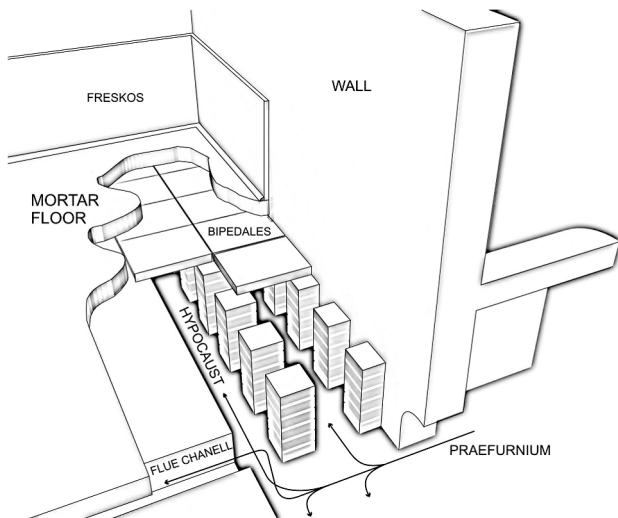


Figure 2 Perspective section through the construction of hypocaust in room W-24a in villa with peristyle in Mediana

## 2 Experimental

### 2.1 Materials

The subject of research shown in this paper was the mortar used for construction of floors over the described hypocaust system. Having in mind that these mortars were exposed to temperature variations, and that they had a specific position in the structure, it was interesting to investigate their properties.

A total of seven samples of mortars were collected from the floors in the rooms W22, W24a, E23 i E22, Fig. 1. The samples are marked with designations from MH1 to MH7.

### 2.2 Methodologies

In research of the mortar from the Roman period, as well as of the mortar from ancient times in general, various methods are used. A very thorough review of historic mortars of various uses was given by J. Elsen [6] using polarisation fluorescence microscopy – PFM. Authors concluded that PFM is indispensable as the first

step in the characterisation of ancient mortars, especially the identification of the different inorganic and organic aggregates (inert), the different mineral additions (latent hydraulic), the binder type, the binder-related particles and in the descriptions of the pore structure.

In research of pore size distribution, a large number of authors used mercury intrusion porosimetry [7  $\div$  11]. The results of the porosimetric evaluation of the mortars indicated that the total porosity values varied within a limited range, whereas the pore size distribution was the critical parameter which showed the most significant variations. The microstructures of the investigated products were far from being similar. These differences should be taken into account during the selection process as they are known to strongly affect the overall durability of the intervention with respect to salt decay.

A significant number of authors used multiple methods in their research in order to obtain as much information as possible. Very often, the following methods are combined: X-ray diffraction analysis (XRD), optical microscopy and scanning electron microscopy (SEM) [12  $\div$  15]. By analyzing the testing results obtained by these methods, the mineral crystalline phase of the mortar was identified. It was determined that almost all of the mortars were made of two phases of clacite and vaterite and the small quantity of quartz, while in certain samples of the mortar there was presence of gypsum and clay material.

Cesare Fiori and his co-workers, as well as many other authors also added thermo-differential DTA and thermogravimetric TGA analysis [16  $\div$  18] to the previously mentioned ones. TGA provides evidence of the presence of portlandite which cannot be determined by wet chemical analysis. In addition, with these two analytical techniques, mineral phases related to the binder and sand fractions can be determined, allowing better identification of the mortar constituents. The amorphous phases coming from hydration and pozzolanic reactions are very difficult to detect or are even not detectable, XRD was complemented with thermogravimetric analysis (TGA) and differential thermogravimetric analysis (DTG) which can identify these reaction products as well as the degree of carbonation and hydration reactions.

For investigation of macro-porosity of the archaeological and historical mortars also the visual procedure using image analysis [19] and flatbed scanners [20] can be used. The studies have proved that it is possible to obtain preliminary quantitative information regarding the macro-porosity of a mortar using a simple flatbed scanner. The images achieved by this system, besides documenting the possible presence of dissolution phenomena of the carbonatic binder, can be used as a basis to extract morphometric information.

Bulk density and real density of the mortar are determined according to the provisions of the standard SRPS B.B8.032:1980. Prior to testing the volumetric mass the samples of mortar are dried up to the constant mass at the temperature  $105 \pm 5$  °C. After cooling down to the temperature of 20 °C the mortar samples are saturated with water using gradual immersion method, to the constant mass, too, according to SRPS B.B8.032:1980. For determination of the volumetric mass of mortar samples, the hydrostatic balance method (KERN

Germany type 572-49) was used. Specific mass was determined with the aid of pycnometer method (gravimetric method).

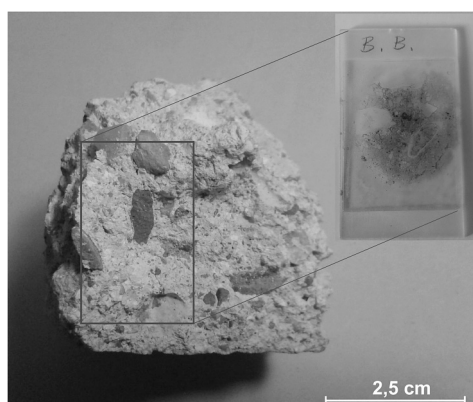


**Figure 3** Macroscopic appearance of the sample MH1 used for creation of preparation for optical tests

In order to determine the mineralogical composition of mortar, i.e. identification of placed aggregate and binder, optical tests were performed on the samples of mortar. The optical tests were performed for the purpose of determining composition, morphology, dimensions of aggregate and binder. The analysis was conducted on the polarization microscope Leica DMLSP, which is connected to the digital camera Leica DC 300. On a separate part of the sample is performed firstly the macroscopic observation of the fragments present in the mortar. Due to the fact that the samples were crumbling, in order to make a petrographic preparation for optical tests, the sample is subjected to impregnation with epoxy-resin in order to bind the ingredients which have heterogeneous composition and hardness. After impregnation and polishing of the sample surface, a preparation was created, which was further used for optical investigation, Fig. 3.

The general aspect of microstructure of mortar samples (examination of morphology and phase composition) and the chemical composition is analysed applying the scanning electronic microscope, model SEM JEOL JSM-6610LV (magnification up to 300 000 times). The tests were performed on the freshly broken (unpolished) surfaces of the samples, as well as on the samples with the polished surface. When testing the unpolished specimens, their surface was plated with the layer of gold (15 to 25 nm) for the purpose of making prominent the edges, pores and other morphological features of mortar. The polished surface was covered with carbon, which is better suited for the purpose than gold, because it yields only one peak during the chemical analysis. This minimized the possibility of overlapping with the peaks of some other element in the analysed sample.

For X-ray analysis test, the powder diffractometer PHILIPS PW 1710 was used. The radiation from the copper anticathode having wavelength  $\text{CuK}\alpha = 1,54178 \text{ \AA}$  was used. The graphite monochromator was used. The working voltage in the tube was  $U = 40 \text{ kV}$ , intensity  $I = 30 \text{ mA}$ . The specimen was examined under the following experimental conditions: range of diffraction angles  $5 - 70^\circ 2\theta$  with the step of  $0,03^\circ$  and time retention of 2 s at

each step. The obtained data of positions of diffraction maximums ( $2\theta/\text{°}$ ) as well as the corresponding intensities were graphically displayed. Based on the obtained values, and comparing to literature data and JCPDS database, the existing crystal phases were identified.

### 3 Results and discussion

The test results of bulk density ( $\gamma$ ), real density ( $\gamma_r$ ), total porosity ( $\alpha$ ) and water absorption by mass ( $H_m$ ) for all seven samples are given in Tab. 1. In the same table are given their average values.

**Table 1** Basic physical characteristics of the tested samples of mortars

Sample designation	Bulk density $\gamma / \text{g/cm}^3$	Real density $\gamma_r / \text{g/cm}^3$	Water absorption $H_m / \%$	Total porosity $\alpha / \%$
MH1	1,73	2,52	18,2	31,3
MH2	1,69	2,51	20,1	32,7
MH3	1,71	2,57	19,2	33,5
MH4	1,68	2,53	20,0	33,6
MH5	1,68	2,49	20,4	32,5
MH6	1,69	2,50	19,6	32,4
MH7	1,65	2,53	21,4	34,8
Average	1,69	2,52	19,8	33,0

Results of tests of basic physical characteristics presented in Tab. 1 show that the average value of bulk density is  $1,69 \text{ g/cm}^3$ . Departure of the lowest result of bulk density from the mentioned average value is 2,37 %, and it is also the departure of the maximum value found.

The average value of real density is  $2,52 \text{ g/cm}^3$ , whereby the deviations of minimum and maximum values are 1,19 % and 1,98 % respectively. On the basis of the value of real and bulk density the total porosity is calculated and its average value is 33,0 %. Deviation of minimum and maximum value of total porosity is 5,15 % and 5,45 %, respectively. On the basis of such high value of total porosity, significant water absorption was expected. It was no less than 18,2 % and no higher than 21,4 %, which is on average 19,8 % for all seven mortar samples. Such results indicate a significant presence of capillary pores, but also the presence of large open pores which are not capillary. The latter were very easy to observe on the surfaces where the mortar was broken, using microscopic sample examination.

The optical examination of macroscopic appearance of the mortar sample showed that it was made up of the aggregate and binder clasts. The clasts and fragments of aggregate are heterogeneous in composition and colour, while the binder is of uniform gray colour, of a carbonate composition, (violent chemical reaction with diluted hydrochloric acid –  $\text{HCl} 1:3$ ), Fig. 4b. Visual observation, among the embedded fragments of the aggregate, reveals quartz, bricks and limestone, Fig. 4a.

The clasts and fragments of bricks are brown to reddish colour, subround to subangular, having maximum dimensions  $4 \times 8 \text{ mm}$ , Fig. 4a. They are most frequently present in the fragments having dimensions  $1 \times 3 \text{ mm}$ . The quartz clasts are gray. Large clasts having cubic forms and dimensions of up to 1 cm are rounded and subrounded, while the finer (broken) fragments are most often angular to subangular, having dimensions up to 2

mm. The limestone clasts are gray to brown colour, and they react violently in contact with the hydrochloric acid, and they are dominantly present in rounded clasts having dimensions up to 2 mm, and sporadically in large clasts having dimensions over  $10 \times 7$  mm. The binder is of light gray colour, porous, crumbling and loose. The violent reaction with diluted hydrochloric acid indicates a carbonate composition of binder, Fig. 4b.

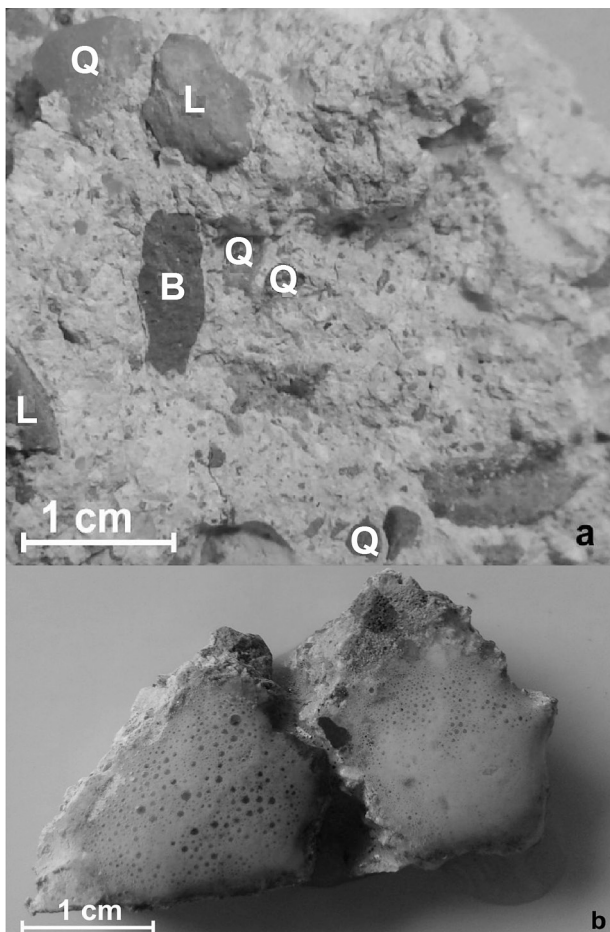


**Figure 4** Mortar sample MH1: a) Brick (B), quartz (Q) and limestone fragments (L) in the historic mortar sample; b) violent reaction of the binder in contact with HCl 1:3

Microscopic examination confirmed that the mortar is made of lithologically heterogeneous clasts (brick, limestone, quartzite/quartz, schist, vulcanite) and homogeneous carbonate binder. Among the clasts of anthropogenic origin, one may mark the presence of broken brick fragments. The brick clasts are subrounded and angular, having dimensions  $2 \times 0,5$  mm to  $0,1 \times 0,2$  mm. In the brown-red matrix of the brick, one may observe a significant presence of fine fraction of the clast, i.e. angular grains of quartz, of light gray interfering colours, having dimensions  $0,05 \times 0,1$  mm, Figs. 5a and 5b. In the matrix, there are fragments of polymimetallic aggregates of quartz, having size  $0,6 \times 0,4$  mm. In the brick fragments, there are isolated oval pores, most often having diameter 0,1 mm (made probably as a result of the loss of clast). Around the brick fragments, a reaction rim can be observed, which was created as a consequence of a chemical reaction with the carbonate binder. The volume share of brick clast is up to 7 %.

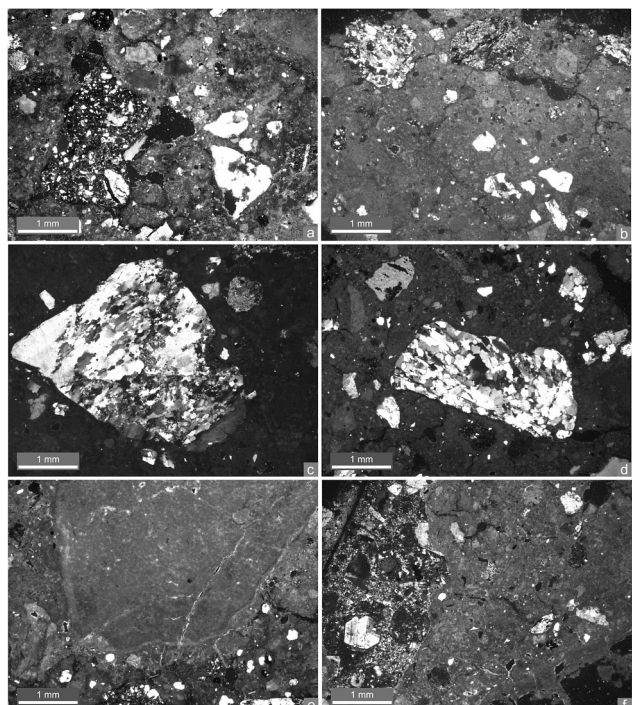


**Figure 5** Microscopic appearance of mortar: a) brick fragment (left half of the figure); b) brick fragment (upper part of the figure); c, d) clasts of polymimetallic aggregate of quartz/quartzite; e) Limestone clast; f) Volcanic rock clasts (left half of the figure)

The limestone clasts represent the most dominant lithological type in the examined sample of historical mortar. There are rounded to subrounded ones, having dimensions even over 1 cm, Fig. 5e, but in significantly smaller subangular to angular fragments, rarely having dimensions greater than  $0,5 \times 0,3$  mm. The coarse clasts indicate presence of micritic limestone, while the fine fragments were recrystallized to different degrees, so all kinds of transitions from micrite to microsparite and sparite can be found. Also the individual self-faced calcite grains having dimensions up to 0,3 mm were found. The presence of limestone clast is up to 25 % of sample volume.

The quartz/quartzite clasts are in terms of volume shear next to the limestone clasts. They occur in large subangular to angular forms, having dimension up to  $4 \times 2$  mm when they represent polymimetallic aggregates of quartz, an/or quartzite fragments (Figs. 5c and 5d) and in finer, monomineral angular fragments with characteristic wavelike blackout, of most frequent dimensions  $0,2 \times 0,1$  mm.

The schist clasts occur in flattened elongated and rounded forms having dimensions  $0,3 \times 0,1$  mm and 0,5 to 0,15 mm. They were created, apart from quartz grains, also of flakes of muscovite, chlorite and in rare instances of biotite of expressed directed orientation which is the main characteristic of textures of metamorphic rocks. In the metamorphic clasts, with the dominant presence of quartz and low expressed schistosity of mica, the presence of isotropic metallic minerals is marked. Apart from the mentioned materials, the rare presence of feldspar leads to conclusion that except schist, the gneiss clast presence is possible. The metamorphic volume share is up to 5 %.

In the mortar aggregate, the optical observation observed the presence of igneous rock fragments, Fig. 5f. It occurs in subangular forms having dimensions  $5 \times 2,5$

mm, with clearly prominent holocrystalline porphyric structure. It is composed of phenocrystals of quartz, plagioclase, hornblende and biotite embedded in the basic mass of quartz and plagioclase. It constitutes up to 2 % of volume of the examined mortar.

Apart from the mentioned ingredients in the aggregate fraction, individual grains of plagioclase, angular forms, of laminar constitution and dimensions up to  $0,15 \times 0,3$  mm constitute up to 1 % of mortar volume.

The binder is homogeneous, brown, having carbonate ( $\text{CaCO}_3$ ) composition.

In the tested sample, the porous system represented by the pores and micro-cracks is very prominent. The pores are most frequently isolated, having oval and elliptic forms having diameter up to 0,3 mm. The micro-cracks are more often empty or filled with ferrous or clay material. They occur along the contacts of the fragments and the binder, and the average width is up to 0,02 mm.

SEM analysis can give valuable information about the mortars materials: binder, aggregates and reaction products. It also facilitates the observation of their shapes, sizes, textures and distribution in the mortars.

In Tab. 2 is presented the average oxide composition determined in the mortar samples with the polished surface.

**Table 2** Average chemical composition of mortar

Weight / %	Sample mark						
	MH1	MH2	MH3	MH4	MH5	MH6	MH7
$\text{Na}_2\text{O}$	1,05	0,15	1,91	2,93	0,36	2,28	0,14
$\text{MgO}$	1,98	1,50	1,50	1,61	0,48	0,65	0,22
$\text{Al}_2\text{O}_3$	6,60	0,59	5,40	12,43	3,69	3,84	0,28
$\text{SiO}_2$	47,65	42,25	34,91	50,42	27,63	54,28	34,83
$\text{P}_2\text{O}_5$	2,80	0,0	0,0	0,0	0,0	0,0	0,0
$\text{SO}_3$	0,59	0,13	0,31	0,20	6,09	0,35	0,21

The results presented in Tab. 2 confirm that it is a lime mortar, in which crushed limestone was used as aggregate (originating from the nearby Sicevo Gorge), river aggregate (from the river Nisava which is in the immediate vicinity of the Mediana site) and crushed brick.

Mineral  $\text{P}_2\text{O}_5$  which is found in the composition of the MH1 sample can be defined as an accidentally present constituent, as it could not be found in the composition of other samples.

In Fig. 6 is presented the characteristic appearance of mortar microstructure (sample MH1 from Tab. 2). On the basis of characteristic excitation of wavelengths of elements found in the given sample (EDS analysis) presence of the following materials was determined: lime binder, crushed bricks, quartz grains and lime grains. In the same figure, the pores (prevailing capillary) of various diameters are clearly observable, as well as micro-cracks.

In the micro-structural composition of lime binder, the SEM analysis (on the freshly broken sample) showed the presence of a large number of micro-pores, Fig. 7.

The bond between the lime binder and aggregate grains is mostly weak, Fig. 8. At the contact of the aggregate grains and binder are formed the transit zones enabling transport of water through mortar, in a capillary

way (through the capillary network). There are some exceptions at the contact zones, on the contact of lime binder and crushed brick grains, where certain chemism took place.

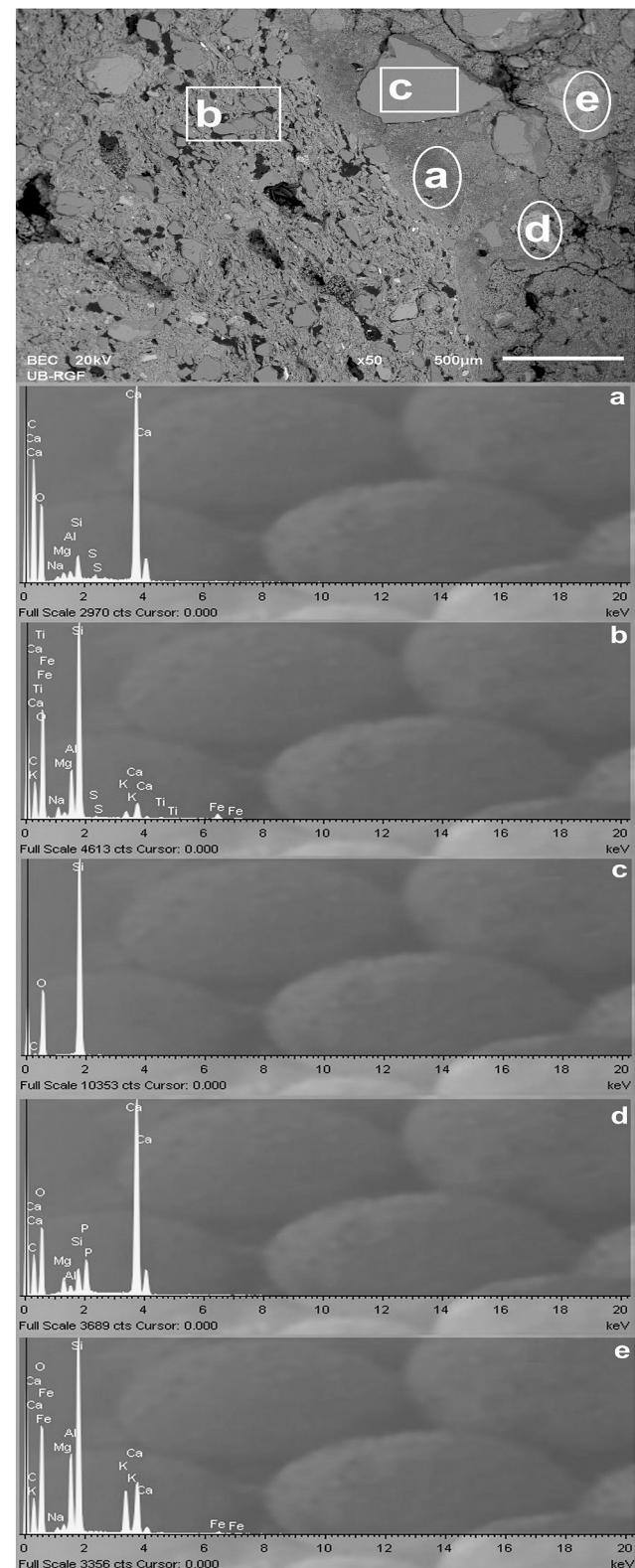


**Figure 6** SEM-EDS observation of mortar samples (MH1) regarding the study of microstructural characteristics: a – binder, b – brick, c – quartz, d – limestone, e – mineral from the amphibole group

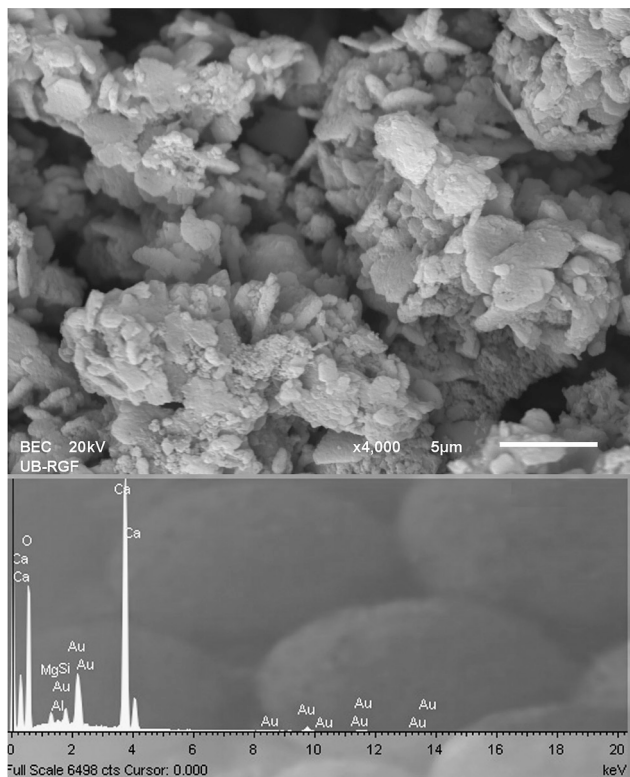


**Figure 7** SEM-EDS image of lime binder, with the visible presence of micro-pores

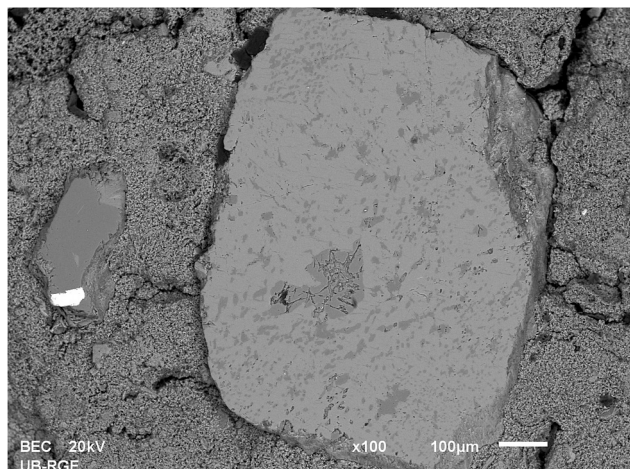


**Figure 8** An example of weak contact between the sand grains (of igneous origin, orthoclase mineral) and binders in mortar

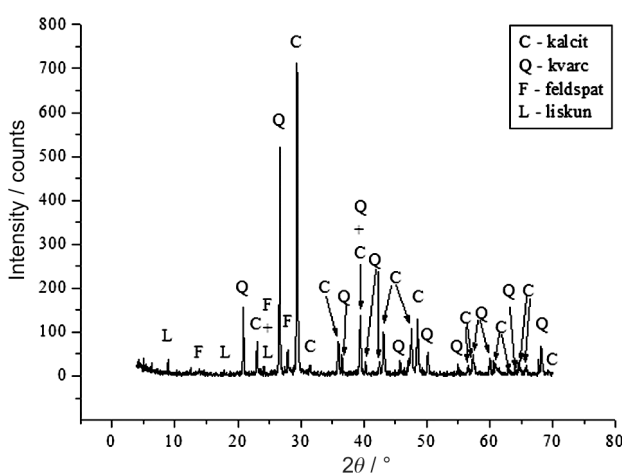


**Figure 9** Mortar sample MH2 - XRD spectrum

XRD analysis in mortar identified multiple crystalline phases. The most present minerals are quartz ( $\text{SiO}_2$ ) and calcite/dolomite (carbonate Ca and Mg). There are small amounts in the group of feldspars (aluminosilicate containing cations of alkali and alkaline earth metals) as well as mica, Fig. 9.

#### 4 Conclusion

Based on the results of tests of physical characteristics it can be conclude that the examined mortar has fairly uniform properties across the entire surface above the hypocaust.

The porosity of mortar is very high and averaged 33,0 %. A major part of those pores were capillary, as confirmed by SEM analysis. According to that, the mortar had a significant water absorption amounting to 19,8 %.

The examined sample of mortar is dominantly composed of carbonate binder and aggregate whose dimensions correspond to the sand fraction (from 0,05 to 2 mm) with the rare occurrence of clasts having dimensions over 10 mm (to 3 % of volume).

The clasts have a heterogeneous composition, and they are represented by the fragments of crushed brick (around 7 % of vol.), limestone (around 25 % of vol.), quartz/quartzite, metamorphite (around 5 % of vol.) and vulcanite (around 2 % vol.). The aggregate is bound by carbonate binder which characterizes the examined sample as lime mortar. Usage of crushed brick and presence of reaction rim confirms the function of hydraulic binding in the examined historic mortar.

The bond of lime binder and aggregate grains is fairly weak, and it is characterized by formed transit zones which facilitate transport of water through mortar through the capillary pores.

The composition of the investigated mortar from the Mediana site is compliant to the historical mortars from other sites of this period. Some Roman mortars from other sites contain puzzolana which is not the case with the investigated mortar, and it is accounted for by the absence of volcanic ash in the Mediana area. The same can be stated for the absence of gypsum.

The performed characterization of the Roman mortar from the Mediana site represents a good starting ground for making the mortar of a compatible composition and properties which can be used for restoration works on the mentioned site.

#### Acknowledgements

The work reported in this paper is a part of the investigation within the research project TR 36017 "Utilization of by-products and recycled waste materials in concrete composites in the scope of sustainable construction development in Serbia: investigation and environmental assessment of possible applications", supported by the Ministry for Science and Technology, Republic of Serbia. This support is gratefully acknowledged.

## 5 References

- [1] Milošević, G. Roman Naissus between the archaeological park and modern town: the archaeological park "Mediana", // Proceedings of the 21<sup>st</sup> International Congress of Byzantine Studies / London, 2006, pp. 281-282.
- [2] Kanitz, F. Römische Studien in Serbien, Wien, 1892., pp. 114-115.
- [3] Milošević, G. Domus and villae urbanae in Serbia, // DOMUS – Das Haus in den Städten der römischen städte in Noricum und Pannonien (Hrs. Peter Sherre), Österreichisches Archäologisches Institut, Sonderschriften band 44 / Wien, 2008, pp. 367-385
- [4] Milošević, G.; Gavrilović, N.; Crnoglavac, V. Condition, Problems and Presentation of the mosaics in Mediana Serbia, // Managing archaeological sites with mosaics: from real problems to practical solutions, The 11<sup>th</sup> Conference for the Conservation of Mosaics (ICCM), Volubilis and Meknes/ Morocco, 2011.
- [5] Bansal, N. K. Characteristic parameters of a hypocaust construction. // Build. Environ. 34 (1999), pp. 305–318.
- [6] Elsen, J. Microscopy of historic mortars – a review. // Cem. Concr. Res. 36, (2006), pp. 1416–1424.
- [7] Klisińska-Kopacz, A.; Tišlova, R.; Adamski, G.; Kozłowski, R. Pore structure of historic and repair Roman cement mortars to establish their compatibility. // J. Cult. Herit. 11, (2010), pp. 404–410.
- [8] Farci, A.; Floris, D.; Meloni, P. Water permeability vs. porosity of Roman mortars. // J. Cult. Herit. 6, (2005), pp. 55–59.
- [9] Silva, D. A.; Wenk, H. R.; Monteiro, P. J. M. Comparative investigation of mortars from Roman Colosseum and cister. // Thermochimica Acta, 438, (2005), pp. 35–40.
- [10] Gulotta, D.; Goidanich, S.; Tedeschi, C.; Nijland, T.; Toniolo, L. Commercial NHL-containing mortars for the preservation of historical architecture. Part 1: Compositional and mechanical characterisation. // Constr. Build. Mater. 39, (2013), pp. 31–42.
- [11] Stefanidou, M. Methods for porosity measurement in lime-based mortars. // Constr. Build. Mater. 24, (2010), pp. 2572–2578.
- [12] Robador, M. D.; Arroyo, F. Characterisation of Roman coatings from the Roman house in Merida (Spain). // J. Cult. Herit. (2013), <http://dx.doi.org/10.1016/j.culher.2012.11.023>.
- [13] Fiori, C.; Vandini, M.; Prati, S.; Chiavari, G. Vaterite in the mortars of mosaic in the Saint Peter basilica, Vatican (Rome). // J. Cult. Herit. 10, (2009), pp. 248–257.
- [14] Binici, H.; Arocena, J.; Kapur, S.; Aksogan, O.; Kaplan, H. Investigation of the physico-chemical and microscopic properties of Ottoman mortars from Erzurum (Turkey). // Constr. Build. Mater. 24, (2010), pp. 1995–2002.
- [15] Yaseen, I. A. B.; Al-Amoush, H.; Al-Farajat, M.; Mayyas, A. Petrography and mineralogy of Roman mortars from buildings of the ancient city Jerash, Jordan. // Constr. Build. Mater. 38, (2013), pp. 465–471.
- [16] Papayianni, I.; Pachta, V.; Stefanidou, M. Analysis of ancient mortars and design of compatible repair mortars: The case study of Odeion of the archaeological site of Dion. // Constr. Build. Mater. 40, (2013), pp. 84–92.
- [17] Drdácký, M.; Fratini, F.; Frankeová, D.; Slížková, Z. The Roman mortars used in the construction of the Ponte di Augusto (Narni, Italy) – A comprehensive assessment. // Constr. Build. Mater. 38, (2013), pp. 1117–1128.
- [18] Schueremans, L.; Cizer, Ö.; Janssens, E.; Serré, G.; Van Balen, K. Characterization of repair mortars for the assessment of their compatibility in restoration projects: Research and practice. // Constr. Build. Mater. 25, (2011), pp. 4338–4350.
- [19] Toplicic-Curcic, G.; Grdic, Z.; Ristic, N.; Despotovic, I.; Djordjevic, D.; Djordjevic, M. Aggregate Type Impact on Water Permeability of Concrete. // Romanian Journal of Materials, 42, 2(2012), pp. 134–142.
- [20] Miriello, D.; Crisci, G. M. Image analysis and flatbed scanners. A visual procedure in order to study the macro-porosity of the archeological and historical mortars. // J. Cult. Herit. 7, (2006), pp. 186–192.

### Authors' addresses

**Gordana A. Topličić-Ćurčić, Ph.D., assistant prof.**

University of Nis,  
Faculty of Civil Engineering and Architecture,  
Aleksandra Medvedeva 14 Street, 18000, Nis, Serbia  
E-mail: gordana.toplicic.curcic@gaf.ni.ac.rs

**Zoran J. Grdić, Ph.D., full prof.**

University of Nis,  
Faculty of Civil Engineering and Architecture,  
Aleksandra Medvedeva 14 Street, 18000, Nis, Serbia  
E-mail: zoran.grdic@gaf.ni.ac.rs

**Nenad S. Ristić, MScCE, assistant lecturer**

University of Nis,  
Faculty of Civil Engineering and Architecture,  
Aleksandra Medvedeva 14 Street, 18000, Nis, Serbia  
E-mail: nenad.ristic@gaf.ni.ac.rs

**Dušan Z. Grdić, MScCE, lecturer**

University of Nis,  
Faculty of Civil Engineering and Architecture,  
Aleksandra Medvedeva 14 Street, 18000, Nis, Serbia  
E-mail: dusan.grdic@hotmail.rs

**Petar B. Mitković, Ph.D., full prof.**

University of Nis,  
Faculty of Civil Engineering and Architecture,  
Aleksandra Medvedeva 14 Street, 18000, Nis, Serbia  
E-mail: petar.mitkovic@gaf.ni.ac.rs

**Igor S. Bjelić, MScCE, lecturer**

University of Nis,  
Faculty of Civil Engineering and Architecture,  
Aleksandra Medvedeva 14 Street, 18000, Nis, Serbia  
E-mail: igor\_bjelic@yahoo.com

**Ana J. Momčilović-Petronijević, MScCE, assistant lecturer,**

University of Nis,  
Faculty of Civil Engineering and Architecture,  
Aleksandra Medvedeva 14 Street, 18000, Nis, Serbia  
E-mail: ana.momcillovic.petronijevic@gaf.ni.ac.rs